

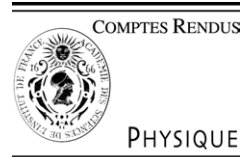


ELSEVIER

Available online at www.sciencedirect.com



C. R. Physique 6 (2005) 399–414



<http://france.elsevier.com/direct/COMREN/>

Aircraft trailing vortices/Tourbillons de sillages d'avions

Unsteadiness, instability and turbulence in trailing vortices

Laurent Jacquin ^{a,*}, David Fabre ^b, Denis Sipp ^a, Eric Coustols ^c

^a ONERA/DAFE, Fundamental and Experimental Aerodynamics Department, 8, rue des Vertugadins, 92190 Meudon, France

^b IMFT, Institut de Mécanique des Fluides de Toulouse, allée du Professeur Camille-Soula, 31400 Toulouse, France

^c ONERA/DMAE, Aerodynamics and Energetics Modelling Department, 2, avenue Edouard-Belin, 31055 Toulouse cedex, France

Available online 14 July 2005

Abstract

This paper is a review on the dynamics of vortices in fluids which get involved in aircraft wakes. Basic notions useful to appraise their dynamics are: inertial waves, 3D instabilities due to vortex interaction, vortex merging, vortex breakdown and turbulence. Each one of these topics is illustrated by means of experimental or numerical results. **To cite this article: L. Jacquin et al., C. R. Physique 6 (2005).**

© 2005 Académie des sciences. Published by Elsevier SAS. All rights reserved.

Résumé

Dynamique des sillages tourbillonnaires : instationnarité, instabilité et turbulence. On effectue une revue des propriétés dynamiques des tourbillons qui se forment dans les sillages d'ailes d'avions. Les notions importantes permettant d'appréhender ces écoulements sur un plan physique sont : les ondes d'inertie, les instabilités hydrodynamiques tridimensionnelles résultant des interactions entre tourbillons, la fusion de tourbillons, l'éclatement tourbillonnaire et la turbulence. Toutes ces notions sont discutées sur la base de résultats théoriques, expérimentaux ou numériques. **Pour citer cet article : L. Jacquin et al., C. R. Physique 6 (2005).**

© 2005 Académie des sciences. Published by Elsevier SAS. All rights reserved.

Keywords: Vortices; Hydrodynamic instability; Turbulence; Aerodynamics

Mots-clés: Tourbillons ; Instabilités hydrodynamiques ; Turbulence ; Aérodynamique

1. Introduction

This paper considers the dynamics of vortices, such as those found behind an aircraft. Important notions, namely inertial waves, stability of vortex flows, and turbulence in vortices, are discussed and are illustrated by means of experimental or numerical results. Section 2 is devoted to the so-called Kelvin waves on which the dynamics of vortices strongly depend. Classical results on the Kelvin waves are recalled and recent results on the properties of these waves in viscous vortices are detailed. Sections 3 and 4 describe the so-called cooperative instabilities which develop in vortex systems due to interaction between the vortices. These instabilities concern both short and long wavelengths and are generic to many applications in fluid mechanics. Indeed, they are largely responsible for the different flow regimes observed in an aircraft wake. For instance, short-wave cooperative instabilities contribute to the vortex merging phenomenon which leads to a reduction in the number

* Corresponding author.

E-mail address: jacquin@onera.fr (L. Jacquin).

of vortices in the near-field behind the aircraft. The physics of vortex merging is detailed in the present issue in the paper by Meunier et al. [1]. Other cooperative instabilities, which are long-wave instabilities, lead to the collapse of the final vortices obtained in the far-field. Section 5 scrutinizes the impact of an axial component of the velocity field. This component is always present in aircraft trailing vortices even if it is usually small. The modifications in the stability properties of the vortex are described and numerical simulations are then used to discuss turbulent aspects. We show that such flows are very resistant to turbulence diffusion compared to other shear flows where rotation is absent. The problem of the mixing of a jet with a vortex, which intervenes in the formation of aircraft contrails (see the papers by Paoli and Garnier [2] and by Schumann [3] in the present issue), provides a good illustration of this resistant nature of vortices to turbulence; this is discussed in Section 7. Before that, Section 6 contains a short review on vortex breakdown, a fascinating mechanism which occurs in vortices when the axial flow becomes strong enough. Section 8 is devoted to a phenomenon called ‘vortex meandering’ which still escapes our understanding in spite of its universal character. The paper ends with a summary of the main results of this review.

2. Waves

Any perturbation in a rotating flow leads to propagation of dispersive waves, called inertia waves. These waves are equivalent to the gravity waves found in stably stratified flows. Those which propagate in a vortex are named Kelvin waves and they play a fundamental role in the dynamics of vortices. The case of a basic flow corresponding to a Rankine vortex (with constant vorticity core) has been extensively described in the literature, see [4,5] for reviews. Recent efforts consider the case of the Lamb–Oseen vortex which is often used to fit real data. The spatial distribution of tangential velocity of the Lamb–Oseen flow can be expressed:

$$V_{\theta}(r) = \frac{\Gamma}{2\pi r} (1 - e^{-r^2/a^2}) \quad (1)$$

where a denotes the vortex radius and $\Gamma = \lim_{r \rightarrow \infty} 2\pi r V_{\theta}(r)$ is the vortex circulation. The Reynolds number is $Re = \Gamma / (2\pi \nu)$. The Kelvin waves in such flows have been described theoretically by following a standard procedure which leads to linearizing the Navier–Stokes equations around the basic flow (1) and considering small modal perturbations of the velocity and pressure of the type $(\underline{v}, p) = (\hat{v}, \hat{p})(r) e^{i(kx + m\theta - \omega t)}$ where $\omega = \omega_r + i\omega_i$ denotes a complex frequency, k is the axial wave number and m , the azimuthal wave number. This leads to an eigenvalue problem for ω . This problem admits a countable infinity of eigenvalues indexed as $\omega_{m,n}(k)$ where k and m are the axial and azimuthal wavenumbers and where the absolute value of second index $|n|$ is related to the number of zeros of the eigenfunction (the higher the label, the more radial oscillations the mode contains). The sign of n is used to distinguish different families of waves. The quantity ω_r/m corresponds to the angular velocity of the wave, and allows to distinguish cograde modes ($\omega_r/m > 1$, the mode rotates faster than the vortex core), retrograde modes ($0 < \omega_r/m < 1$, the mode rotates in the same direction than the vortex core but slower), and counterrotating modes ($\omega_r/m < 0$, the mode rotates in the opposite direction than the vortex core). Results are shown in Fig. 1 for the vortex described by (1). Both the axisymmetric modes $m = 0$ and the helical modes $m = 1$ (left-handed helices) are shown. The frequencies are made non-dimensional with the rotation rate of the vortex center, $\Omega_0 = \Gamma / 2\pi a^2$. A complete classification of these waves is provided by Fabre et al. [6].

2.1. Axisymmetric modes ($m = 0$)

For axisymmetric modes ($m = 0$), see Fig. 1(a), the waves form two families of branches which propagate in opposite directions. The physical mechanism responsible for the propagation of axisymmetric waves has been explained by Melander and Hussain [7] and by Arendt et al. [8]. The group velocity $d\omega_r/dk$, which corresponds to the slope of the different branches, decreases with the wavenumber, the fastest waves being on the branch $\omega_{0,1}$ in the limit of long wavelength ($ka \rightarrow 0$). The group velocity of this wave is found to be $d\omega_{0,1}(k)/dk \approx 0.63\Gamma / (2\pi a)$ which is almost exactly equal to the maximum tangential velocity of the Lamb–Oseen vortex. This means that energy of perturbations propagates with a speed smaller than the maximum tangential velocity of the vortex: $d\omega_{0,n}(k)/dk \leq V_{\theta \max}$, a property which also holds for other vortex models. When $V_{\theta \max} / U_{\infty} < 1$, as found in trailing vortices (with U_{θ} the freestream velocity ahead of the vortex generator), energy of the perturbations is thus convected downstream. This prevents propagation of energy upstream and protects the flow from occurrence of vortex breakdown, as discussed in Section 6.

2.2. Asymmetric modes ($m \neq 0$)

The most robust asymmetric waves are the helical waves $|m| = 1$. Due to the symmetries, they satisfy $\omega_{1,n} = -\omega_{-1,n}$ and they must be considered as pairs, the left-handed modes ($m = 1$) propagating along the vortex core in opposite directions

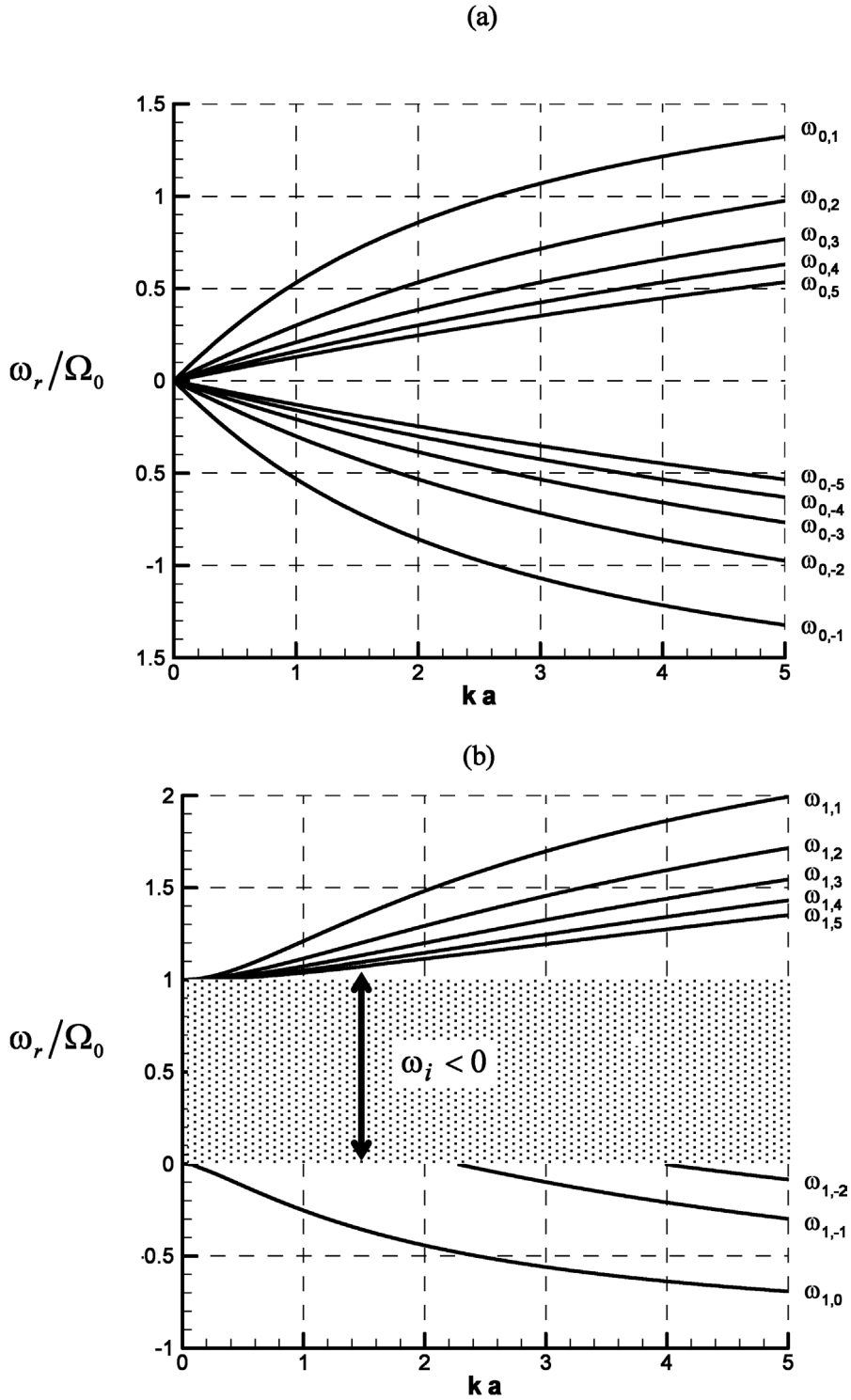


Fig. 1. Lamb–Oseen vortex—inviscid case. Frequencies ω_r of the Kelvin waves: (a) axisymmetric modes $m = 0$, (b) helical modes $m = 1$. Frequencies are normalized by the vortex rotation rate $\Omega_0 = \Gamma/2\pi a^2$, where Γ is the circulation, and a , the vortex core radius. The dotted area is the critical layer region. From [6].

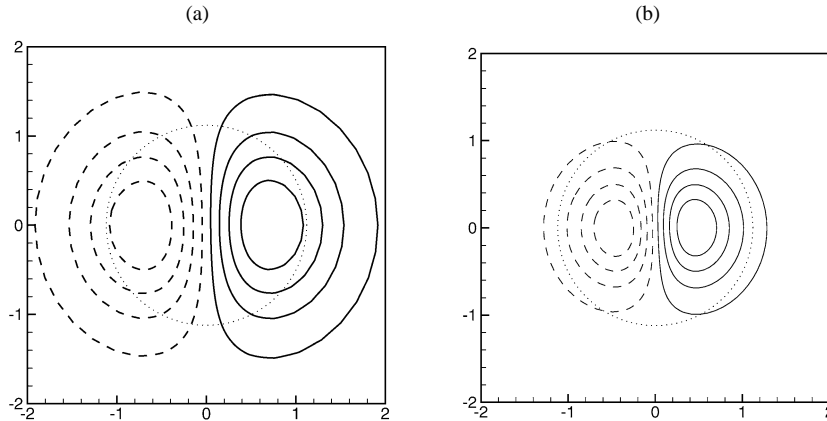


Fig. 2. Lamb–Oseen vortex—viscous case— $Re = 1000$. The ‘slow waves’ ($m = 1, \omega_{1,0}$), see Fig. 1(b), for: (a) $ka = 0.1, \omega/\Omega_0 = -0.012 - 4.710 \times 10^{-5}i$, (b) $ka = 3, \omega/\Omega_0 = -0.5602 - 0.0124i$. Iso-levels of the axial vorticity component in the (x, y) plane. Eight equally spaced levels are displayed, and dashed levels correspond to negative values. The dotted circle corresponds to the location of maximum tangential velocity of the vortex (at $r = 1.1209a$). From [6].

to their right-handed counterparts ($m = -1$). The cylindrical modes described above are weakly dependent on the base flow model. Sensibility to the base flow becomes much more important for $m \neq 0$ and this is due in particular to the presence of critical layers. Critical layers develop whenever the angular phase speed of the perturbation, ω_r/m , coincides with the angular velocity of the vortex $\Omega(r_c)$ at some radius r_c . In this case, computations show that such waves are damped ($\omega_i < 0$): the critical layers have an important effect on the global vortex dynamics because they filter the perturbation spectrum by eliminating all co-rotating waves such that $0 < \omega_r/m < 1$. For $m = 1$, this occurs in a Lamb–Oseen vortex within the dotted area of Fig. 1(b), where $0 < \omega_r < \Omega_0$. Outside this interval, the modes are regular and purely oscillatory ($\omega_i = 0$). Two of these branches are of particular importance in practice:

The branch labeled $\omega_{1,0}$ corresponds to the wave with the simplest structure (eigenfunction with no zero). This wave is counter-rotating, and is called the ‘slow wave’ because both the frequency and the phase velocity $c = \omega_r/k$ (and also the group velocity $d\omega_r/dk$) tend towards zero when k goes to zero. This regular wave takes the form of a helical displacement of the vortex core as a whole and corresponds actually to the self-induced oscillation mode of a filament vortex, see Saffman [4]. As can be observed in Fig. 2, the eigenmode takes the form of a dipole of vorticity. When superposed onto the base flow, the effect of this dipole is to increase the vorticity on one half of the vortex and to decrease it in the other half. Therefore, the net effect corresponds to a displacement of the whole vortex core in a helical way. The mode is weakly dependent on the axial wavenumber (compare Fig. 2(a) and (b)). It is also weakly dependent upon the vortex core details, and it is generic to all vortex models. It plays an important role because it is involved in the long-wave cooperative instabilities that will be considered in Section 3.

Other important branches are those labeled $\omega_{1,-n}$, $n = 1, 2, \dots$, which are counter-rotating neutral waves outside the critical layer region. The transition, where $\omega_r = 0$, correspond to steady waves that play an important role because they can be amplified whenever an external steady strain is imposed on the flow. For a Lamb–Oseen vortex, see Fig. 1(b), the corresponding wavenumbers are found to be $k_c a \approx 2.26, 3.96, 5.61, \dots$. Fig. 3(a) shows the eigenmode corresponding to the first steady wave $k_c a \approx 2.26$. It consists in two vorticity dipoles. The steady nature of this particular mode results from cancellation of the opposite effects by each dipole which, by itself, would displace the core as explained above. The superposition of these $m = 1$ waves with their $m = -1$ counterparts leads to steady untwisted perturbations schematized in Fig. 4 (the figure is obtained for a Rankine vortex for which $\omega_r = 0$ is $k_c a \approx 2.5$ instead of $k_c a \approx 2.26$ for the Lamb–Oseen vortex). Such steady untwisted perturbations are particularly important because they can be amplified by the straining field imposed by other vortices. This mechanism is responsible for the short-wave cooperative instability described in Section 4. As shown in Fig. 3(b), when penetrating the critical region by decreasing ka and following the branch $\omega_{1,-1}$, dramatic modifications in the eigenmode structure occur: two spiral arms develop outside the vortex and wind on with increasing vorticity levels. This spiral structure is the signature of the critical level phenomenon evoked above. Before such structures are eliminated by viscosity they may establish possible communication between the vortex core and its periphery. Their importance on the global dynamics of a vortex is not yet understood.

2.3. The initial value problem

Another approach to characterize the linear dynamics of an isolated vortex, which is complementary to the modal point of view presented above, is to study the response to an initially localized perturbation through a solution of the linear initial

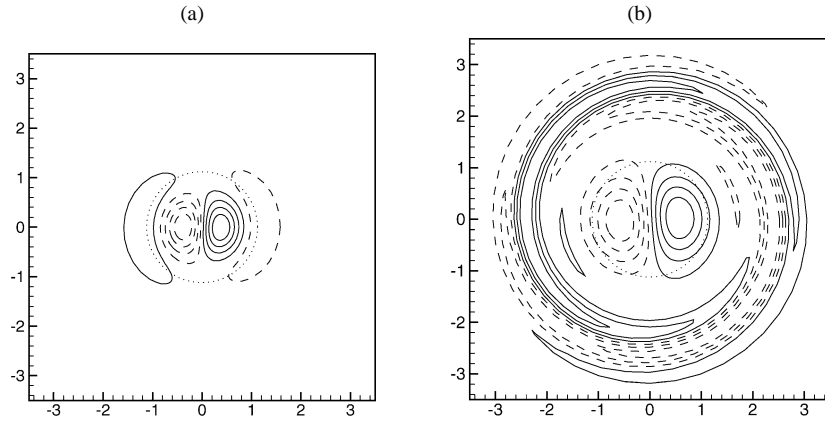


Fig. 3. The bending waves ($m = 1, \omega_{1,-1}$), see Fig. 1(b), for $Re = 1000$: (a) steady mode: $ka = 2.262, \omega/\Omega_0 = -0.0119i$, (b) critical layer mode: $ka = 0.8, \omega/\Omega_0 = 0.1560 - 0.0433i$. Same conventions as in Fig. 2. From [6].

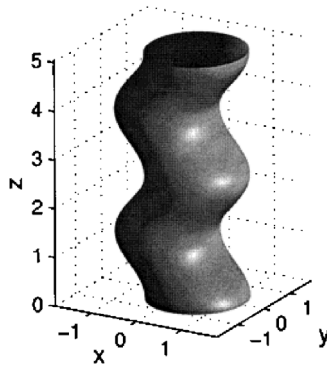


Fig. 4. Wave motion produced by the combination of two steady Kelvin waves $\omega_{1,-1}$ and $\omega_{-1,-1}$ for $ka \approx 2.5$ (Rankine vortex). The vortex core boundary is displayed with an arbitrary amplitude. From [5].

value problem. Such a study was performed by Arendt et al. [8] for the Rankine vortex model. They found that an initially localized perturbation of the vortex core always gives rise to the propagation of wavepackets which propagate the energy of the perturbation along the vortex core. Fabre [9] repeated the same kind of analysis for the Lamb–Oseen vortex. He found that generally, only a part of the initial energy propagates under the form of wavepackets, while another part is rapidly dissipated through a filamentation mechanism. In Fig. 5, we present the results obtained when the initial perturbation takes the form of a ‘helical twist’ of the vortex, defined in order to include only helical, left-handed ($m = 1$) eigencomponents. The Reynolds number is $Re = 1000$. The upper plot shows a three-dimensional view of the axial vorticity component of the initial perturbation. The dark and light areas correspond to regions of positive and negative values. The middle plot shows the perturbation, with the same representation, at an instant corresponding to 10 rotation times of the vortex core, and the lower plot shows three transverse views of the perturbation. As can be observed, this perturbation can be decomposed into three main components. The first one is a twisted perturbation, with a structure essentially similar to that of the initial perturbation, which has propagated to the left. This structure is recognized as a wavepacket corresponding to the displacement wave evoked above. The second component is a structure characterized by the presence of spiral arms in the periphery of the vortex. This structure stays at the initial location of the perturbation without propagating, and decays while it is wrapped. From a modal point of view, this structure is the contribution from the critical layer waves. The third component is a small dipolar structure propagating to the right, which can be recognized as a wavepacket corresponding to the corotating wave labeled $\omega_{1,1}$. Inspection shows that about half of the energy is propagated to the left within the displacement wavepacket, while another half remains in the spiral structure and is rapidly dissipated. The small wavepacket propagating to the right only bears a small fraction of the initial energy. Other kind of initial perturbations were also considered in [9]. For axisymmetric perturbations, all the energy is propagated under the form of wavepackets. On the other hand, for initial perturbations of double-helix ($m = 2$) or more complex geometries, all the energy is rapidly dissipated under the form of a spiral structure, and no propagating wavepacket is observed.

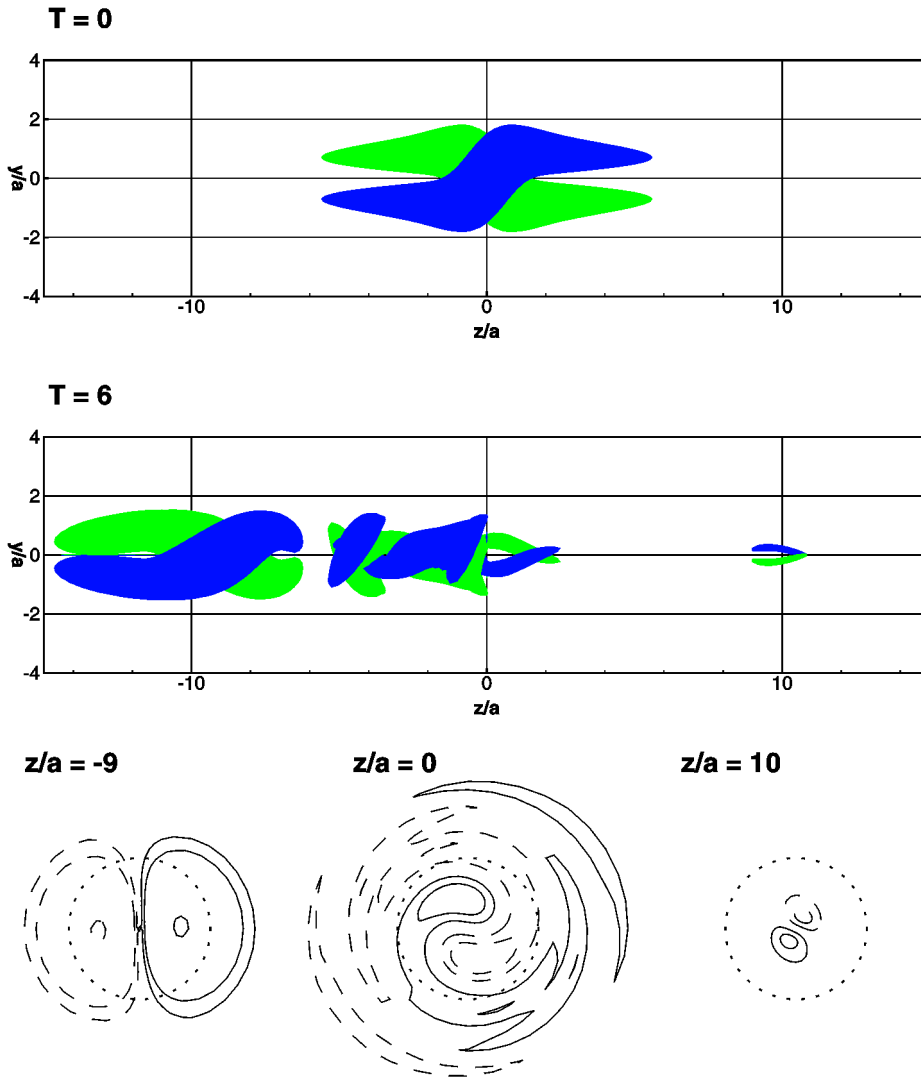


Fig. 5. Response of a Lamb–Oseen vortex to an initially localised perturbation under the form of a “helical twist”. Upper: initial perturbation. Middle: final perturbation after 10 rotation times of the vortex centreline. Lower: transverse structure of the final perturbation at three axial locations. From [9].

3. Long-wave cooperative instabilities

Vortex systems are generally unstable with respect to 3D perturbations. This results from amplification of asymmetric Kelvin waves under mutual straining of the vortices. If separations between the vortices are large compare with their thickness, a system of stability equations may be derived by considering a set of parallel vortex filaments with slight sinusoidal perturbations of their respective positions. The developed expressions of this linear system are given in Crow [10] for the case of a single pair of counter rotating vortex filaments, and in Crouch [11], Fabre et al. [12] for multiple vortex pairs. The system evolves due to superposition of three effects:

- (i) the straining experienced by each filament when displaced by a perturbation from its mean position in the velocity field induced by the other undisturbed filaments,
- (ii) the self induced rotation of the disturbed filament; and
- (iii) the velocity field induced on the filament by the other vortices when they are themselves perturbed from their mean positions, see Crow [10].

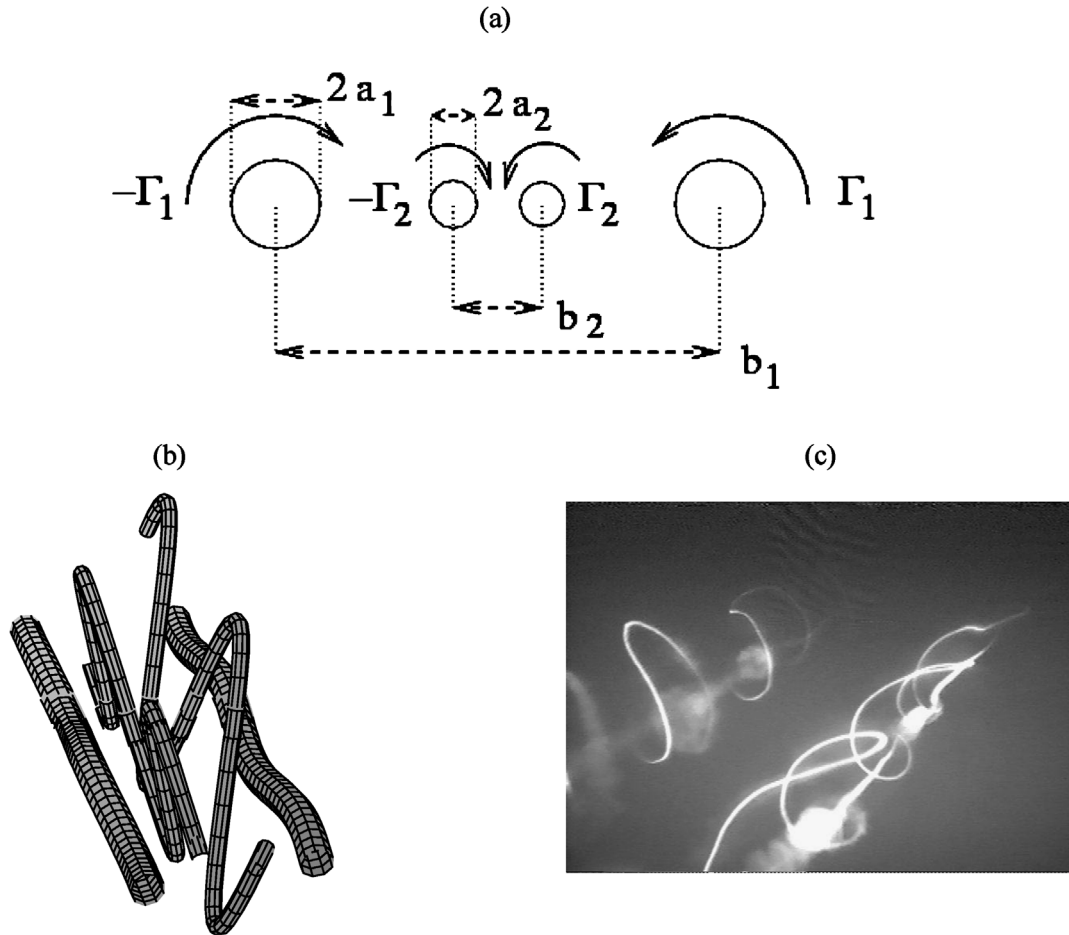


Fig. 6. Long-wave cooperative perturbation in the wake of a wing equipped with flaps: (a) definitions of the four vortex system; (b) optimal perturbation obtained with the linear theory after one revolution of the inner vortex pair around the outer one (case $\Gamma_2/\Gamma_1 = -0.3$, $b_2/b_1 = 0.3$, from [12]); (c) towing tank experiment for $\Gamma_2/\Gamma_1 = -0.37$, $b_2/b_1 = 0.5$. Fig. 6(c) shows the perturbation obtained after an elapsed time close to that corresponding to Fig. 6(b); from [13].

Mechanism (i) leads to amplification of the asymmetric Kelvin waves when their polarization planes remain close to the extension planes of the straining field; this mechanism is in balance with the self induced rotation, mechanism (ii), which tends to shift the perturbation away from these planes. The frequency of this self-induced oscillation is the frequency of the oscillation mode of the Kelvin displacement wave described in Section 2. This is the mechanism which introduces a dependence of the solution with respect to a measure of the vortex core radius.

Long-wave cooperative instabilities are of prime importance for applications to aircraft hazard alleviation because one hopes that the dispersion of a vortex wake may be accelerated by means of this mechanism. The stability properties of a vortex configuration composed with two vortex pairs of opposite sign, as sketched in Fig. 6(a), has been especially considered. The vortex pairs may be co-rotating ($\Gamma_1 > 0$, $\Gamma_2 > 0$) or counter-rotating ($\Gamma_1 > 0$, $\Gamma_2 < 0$). In the wake of an aircraft, the outer vortex pair is that produced at the wing tips and the inner one may be produced by flaps or horizontal tail planes. The linear method evoked above may be applied to the case of Fig. 6(a) if $a_1, a_2 \ll b_1, b_2$, $(b_1 - b_2)/2$; the solution depends on Γ_2/Γ_1 and on b_2/b_1 . Without inner vortices, the classical Crow instability develops on the outer vortex pair. The wave length of the Crow instability is $kb_1 \approx 0.8$ (wavelength $\lambda/b_1 \approx 7.85$) and its growth rate is $\omega_{i,Crow} \approx 0.8\Gamma_1/(2\pi b_1^2)$ [10]. Adding the second vortex pair leads to much higher amplifications [11,12]. Fig. 6(b) shows a result of the linear theory for $\Gamma_2/\Gamma_1 = -0.3$ and $b_2/b_1 = 0.3$ (which may be considered as a limit for an aircraft). The most amplified perturbation has been plotted after one revolution of the inner vortices around the outer ones. This perturbation, introduced initially, has been amplified by a factor 5700, to be compared to 2.2, the value obtained for the Crow instability (without inner vortices). The towing tank result shown in Fig. 6(c) confirms that this type of perturbation is effectively selected in a real four vortex wake, see [13] and the paper by

Savas [14] in the present volume. Differences between the linear solution, Fig. 6(b), and the experiment, Fig. 6(c), are bending of the loops and local burstings. They are due to non-linearity.

4. Short-wave cooperative instabilities

As said above, the presence of a second vortex leads to imposition of a strain field on the current vortex. In a counter-rotating vortex pair of circulation $\pm\Gamma$ separated by a distance b , this strain is at a rate equal to $\Gamma/(2\pi b^2)$. If we consider the flow within the core of each vortex, steady waves such as that described in Fig. 4 are amplified by this strain. When considering the flow evolution on the length and time scales $L = a$ and $T = 2\pi a^2/\Gamma$, the strain amounts to a perturbation at order $\varepsilon = (a/b)^2$; it corresponds to the stream-function $\psi(r, \theta) = -f(r) \cos 2\theta/2$, where the function $f(r)$ must be determined so that the velocity field fulfils the steady Euler equations at order ε , see Moore and Saffman [15]. More generally, considering 3D perturbations, i.e., two Kelvin waves with azimuthal wavenumber m_1, m_2 and with an amplitude $\delta \ll 1$ (normalized by b), interaction leading to instability occurs at the order $\delta \times \varepsilon$ and the mechanism is a global resonant interaction between three steady perturbations, i.e., two Kelvin waves and the strain, which takes place as soon as the triadic resonance relation $m_1 - m_2 = 2$ is satisfied. Thanks to the viscous filtering effect of critical layers (see Section 2), for the Lamb–Oseen vortex this only occurs for $m_1 = 1, m_2 = -1$. The amplification rate ω_i of these cooperative instabilities, as obtained using the Moore and Saffman method, corresponds to a narrow band of instability centered around the wave number k_c such that $\omega_{\pm 1, n}(k_c) = 0$, see Eloy and Le Dizès [16], Sipp and Jacquin [17]. Fig. 7 shows the amplification rate for the instabilities due to resonance of the straining field in a dipole of counter-rotating dipoles of aspect ratio $a/b = 0.208$. Resonance occurs with the steady helical waves ($\omega_r = 0, m = \pm 1, k_c a \approx 2.26, 3.96, 5.61, \dots$), see Fig. 1(b). The amplification rate for these instabilities, called Widnall instabilities, is $\omega_i = 1.4\Gamma/(2\pi b^2)$, which is comparable to that of the Crow instability, $\omega_{i, \text{Crow}} \approx 0.8\Gamma/(2\pi b^2)$. The time scales τ of the two instabilities are thus equivalent and are of the order $O(2\pi b^2/\Gamma)$. Compared with the viscous time scale $\tau_v \propto a^2/\nu$, we have $\tau_v/\tau \propto (a/b)^2 Re$. As a consequence, if $a/b = O(0.1)$ for instance, the cooperative instabilities are free from viscous damping when $Re \gg 100$.

The short-wave cooperative instabilities are of fundamental importance because they are responsible for the merger of vortices in the absence of significant turbulence. Merger occurs on a convective time scale $\omega_i^{-1} \propto 2\pi b^2/\Gamma$ when the vortices come close enough and when the Reynolds number is sufficiently large to allow development of the short-wave instability mechanism. Fig. 8 shows results of a direct numerical simulation of a co-rotating dipole of aspect ratio $a/b = 0.2$ for $Re = 5000$, Le Dizès and Laporte [18] (see the paper by Meunier et al. [1] in the present issue). Contrary to the case of the counter-rotating vortex pair, the strain is now rotating (with the pair). The resonance mechanism described above still holds and leads to the

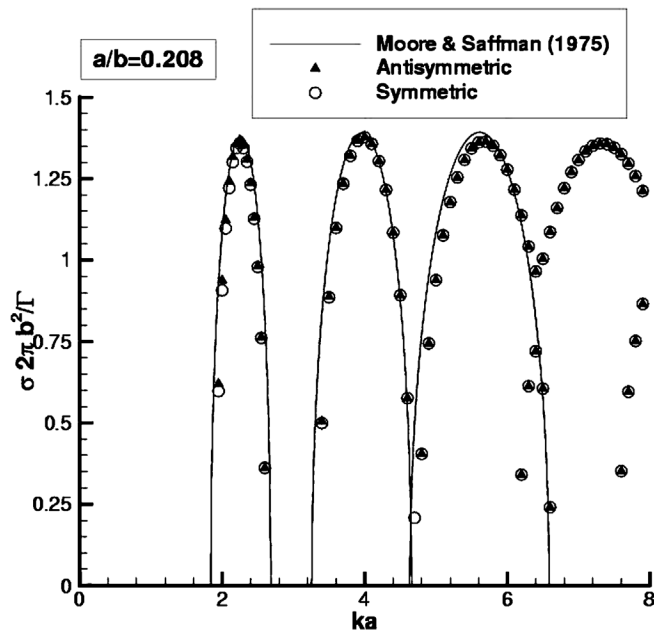


Fig. 7. Amplification rate of the Widnall instabilities for the dipole $a/b = 0.208$ at $Re = \infty$. Lines: asymptotic theory, symbols: matrix eigenvalue method. From [17].

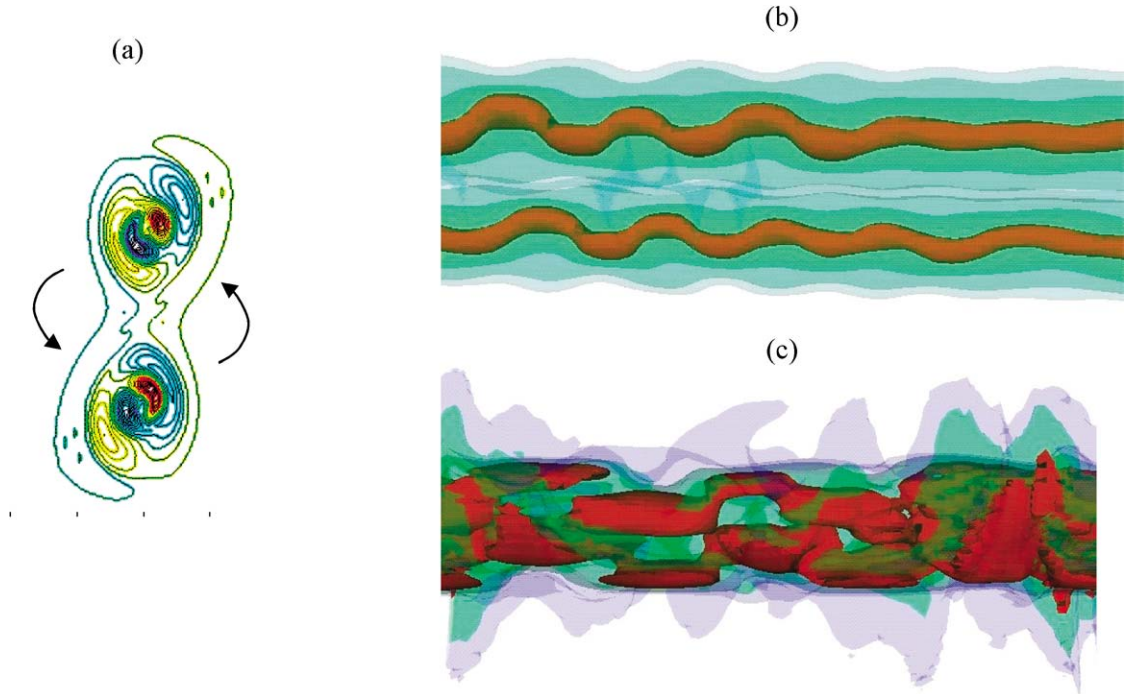


Fig. 8. Iso-levels of the axial vorticity perturbation component in a direct numerical simulation of a co-rotating dipole of aspect ratio $a/b = 0.2$ for $Re = 5000$: (a) cut in the (x, y) plane during the linear regime (compare to Fig. 3(a)), (b) side view during the linear regime, (c) side view during merging. From [18].

same type of growth mechanism. The complete theory is given in [18]. The two vortex cores deform, see Fig. 8(b), and for $a/b = 0.2$ they are sufficiently close to exchange their vorticity; this leads to a strongly non-linear interaction regime during which the two cores merge, see Fig. 8(c). These numerical results are in fair accordance with experiments conducted in a water tank by Meunier and Leweke [19]. Merging needs sufficient proximity between the vortices, an approximate criterion being $a/b > 0.25$ [19]. This limit is likely due to non-linear saturation of the primary instability: when amplitude of the instability becomes too large, self induced rotation tilts the perturbation which escapes away from the stretching directions of the strain. Sipp [20] showed for instance that the wave $k_c a \approx 2.26$ of a counter-rotating dipole is subjected to core displacements Δ which cannot exceed $\Delta/b = 6.1(a/b)^2$. This gives $\Delta/b \approx 0.25$ for the maximum distance of separation required for the merger of a pair of counter-rotating vortices with an aspect ratio $a/b = 0.2$, in excellent agreement with observations made by Leweke and Williamson [21] in their low Reynolds number experiments conducted in a water-tank. This value seems also to hold in co-rotating vortices. Importantly, short-wave cooperative instabilities are thus contributors to the fusion of various vortices in the near-field of an aircraft; they become unimportant in the far-field, when $a/b \ll 1$.

5. Instabilities with axial flow

We consider now the effect of axial flow on a single trailing vortex. Due to the presence of axial shear, instabilities exist which do not occur in the absence of axial flow. They have been extensively studied for the Batchelor vortex which is very often used to fit 3D vortices (see Ash and Khorrami [22] for a review). This model corresponds to a Gaussian axial velocity profile:

$$U(r) = U_0 \pm \Delta U e^{-(r/a)^2} \quad (2)$$

superposed on the Lamb–Oseen vortex (1). The dynamics of this flow are controlled by the swirl number:

$$q = \frac{\Gamma}{2\pi a \Delta U} \approx 1.56 \frac{V_0}{\Delta U} \quad (3)$$

where V_0 is the peak tangential velocity, $V_0 = \max\{V_\theta\}$. Linear stability analysis applied to this flow shows three families of instabilities. The first, which are basically inviscid, are short-wave instabilities due to stretching of vorticity perturbations aligned with the local shear. These instabilities are well described by the asymptotic study of Leibovich and Stewartson [23] which

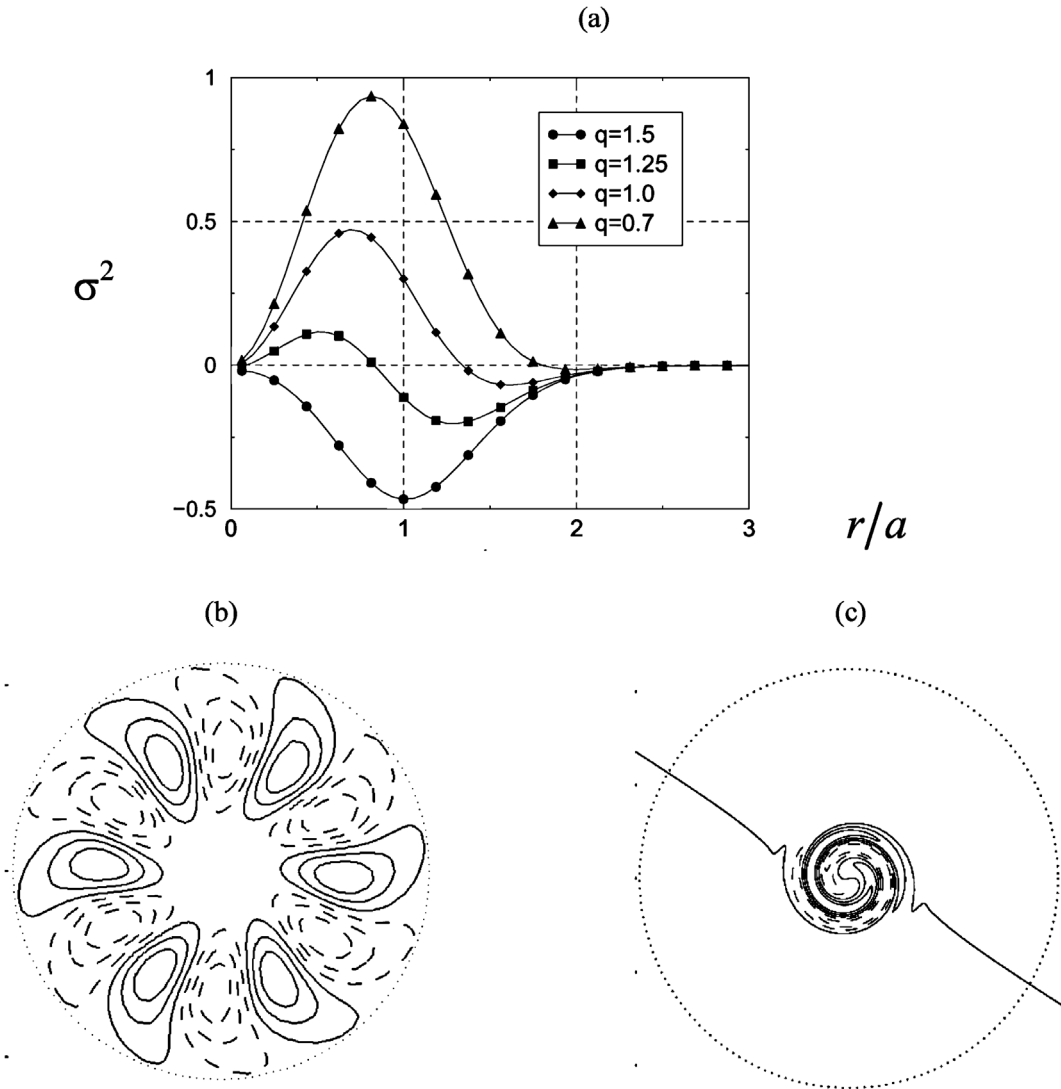


Fig. 9. Instabilities in a Batchelor vortex: (a) amplification factor of the inviscid ‘ring modes’ as a function of the radius for different q , (b) most amplified ‘ring mode’ for $q = 1$, $Re = 2000$ [24], (c) example of unstable ‘centre mode’ for $q = 2$, $Re = 10^5$, $m = -1$ [25]; axial component of vorticity fluctuation are plotted in figure (b) and (c); the broken and solid lines correspond to vorticity of opposite sign; the dotted circles correspond to $r = a$.

leads to a necessary stability criterion generalizing the classical Rayleigh criterion of centrifugal instability. Asymptotic means that the analysis is conducted in the short-wave limit $ka \gg 1$ and $|m| \gg 1$. These short-wave criteria gives the amplification rate σ of the most amplified modes (considering perturbations $\sim e^{\sigma t}$) as function of the radius r . It is plotted in Fig. 9(a) for different values of the swirl number q . When this parameter is positive, the flow is unstable. Fig. 9(a) shows that for $q = 1.5$ the core of the vortex is entirely stabilized ($\sigma^2 < 0, \forall r$); it is fully unstable ($\sigma^2 > 0, \forall r$) for $q = 0.7$. For intermediate values, e.g., $q = 1$, a stable buffer layer where $\sigma^2 < 0$ is surrounding the flow and prevents radial propagation of perturbations. The instability modes in the core take the form of ‘ring-modes’ which exhibit a structure concentrated in an annular region located around the core. An example of such a mode is shown in Fig. 9(b): this is the most amplified mode found for $q = 1$ and $Re = 2000$ (actually a $|m| = 6$ mode). As said above, these modes develop for $q < 1.5$ and above this value, the strong rotation stabilizes all the perturbations. A second instability family is the viscous modes evidenced by Khorrami, see [22]. These modes occur for $q < 1.2$, and their growth rates are several orders of magnitude smaller than those of the inviscid modes occurring in this range. Consequently, they are unlikely to play any role in the dynamics of wake vortices. Finally, a third family are the viscous ‘centre-modes’ recently described by Fabre and Jacquin [25]. These modes exist for very large Reynolds numbers, and for swirl

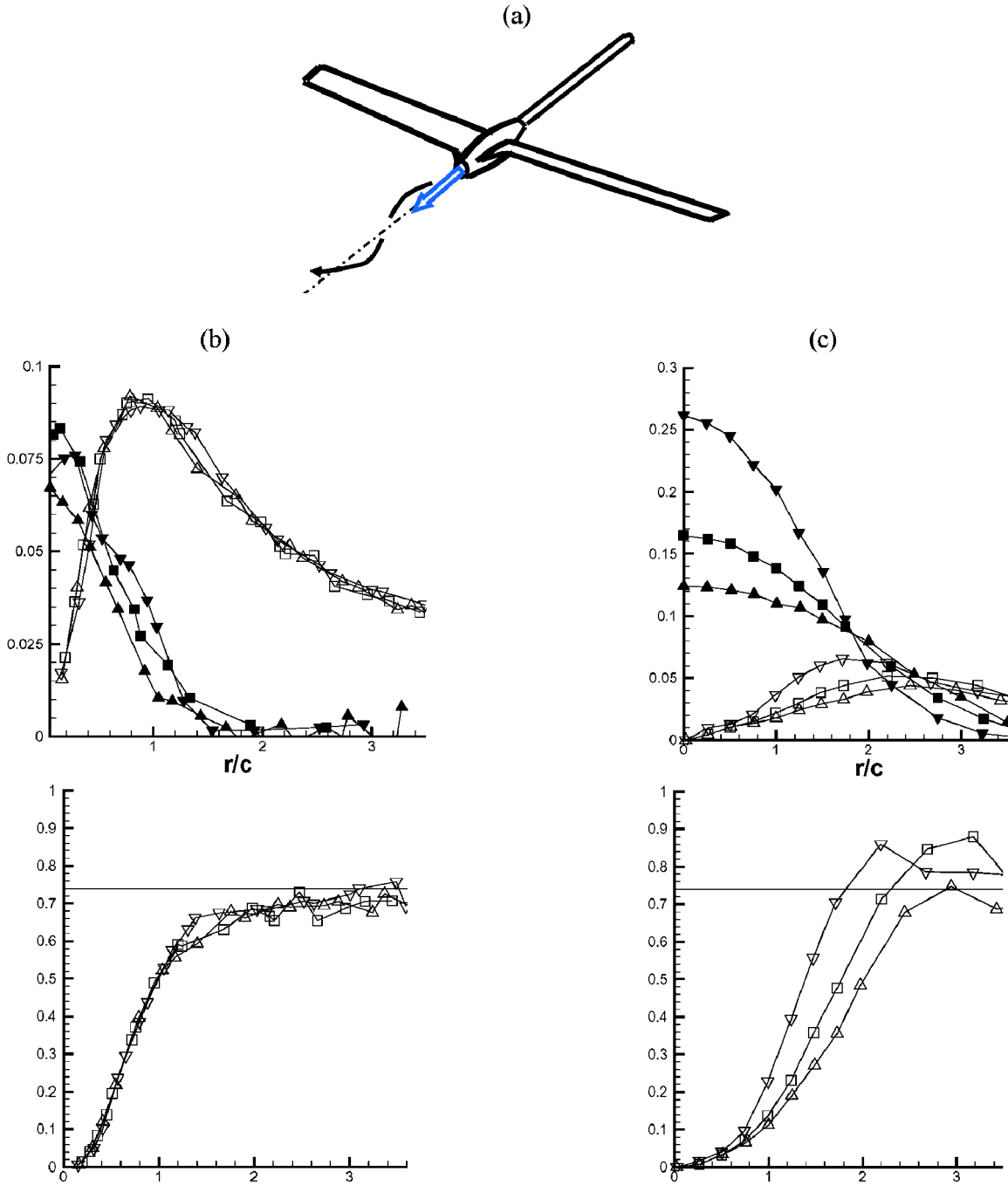


Fig. 10. Jet/vortex experiment [26]: vortex generator (a), radial mean velocity profiles (top: open symbols V_θ/U_∞ , solid symbols $\Delta U/U_\infty$) and circulation (bottom) measured by hot wire in three downstream sections—case of a weak jet (b), case of a strong jet (c). Symbols: \blacktriangledown $z/c = 45$, \blacksquare $z/c = 78$, \blacktriangle $z/c = 109$ with c the wing chord length. Radius is normalized by c . From [24].

numbers much larger than the other families of instabilities. So, they could be present in any trailing vortices. As illustrated in Fig. 9(c) they have the particularity to be strongly localized near the vortex axis. Such instabilities could participate to the ‘vortex meandering’ phenomenon discussed in Section 8 but are likely not efficient to promote turbulence and mixing.

An illustration of some of these mechanisms is provided by the experiment by Phillips and Graham [26] which was revisited by Jacquin and Pantano [24] and which is shown in Fig. 10. This experiment is based on the use of a split wing with a narrow

central cylindrical body, see Fig. 10(a). This apparatus produces a single vortex whose core may be manipulated by blowing a jet or by producing a wake with an obstacle placed in the central body region. Several cases were studied in this reference. Two of them have been selected in Fig. 10. This figure shows radial profiles of the axial velocity difference, ΔU , the tangential velocity, V_θ , and the angular momentum rV_θ , normalized by the free-stream velocity U_∞ and by the wing chord length c . Fig. 10(b) corresponds to the case of a weak jet which is such that $q \approx 1.8$ (using (3)) in the first measurement section. In that case, $q > 1.5$ and the vortex is linearly stable (no ring modes). The measurements confirm that angular momentum of the vortex remains frozen. The jet case shown in Fig. 10(c) corresponds to a stronger jet. Here $q \approx 0.4$ in the first measurement section. The flow is strongly unstable and it is subjected to a vigorous diffusion: ΔU decays and a increases (note that at $x/c = 45$, the vortex core is already twice as large as that of the previous case). The inviscid shear instabilities described above are likely responsible for this behaviour. As for the ‘centre mode’, they could develop in the weak jet case, but they are too confined, see Fig. 9(c), to promote diffusion of the core. The angular momentum in Fig. 10(c) shows that spreading of the jet-vortex is due to a centrifugal instability in the periphery of the vortex. As shown by Jacquin and Pantano [24], this is the results of a breaking of the stabilizing region which confines the shear induced perturbations created in the core at higher swirl numbers. The stability of the vortex periphery inhibits radial transport so that a linearly unstable vortex with moderate swirl number (not too small) becomes turbulent but comes back in a form that is stable without significant changes in the vortex width [24]. Ragab and Sreedhar [27] were the first to observe this striking stability property of the vortices which will be discussed further in Section 7.

6. Vortex breakdown

The vortex breakdown phenomenon is a spectacular effect of the Kelvin waves on the global dynamics of a vortex. As advocated by Benjamin [28,29], vortex breakdown results from a transition from a globally stable and supercritical flow supporting only downstream travelling waves to a subcritical state supporting both upstream and downstream propagating waves. If the flow is subcritical, the Kelvin waves might transport their energy upstream and disrupt the flow. As pointed out by Gallaire and Chomaz [30], this condition is close to an absolute/convective instability condition (a base flow is said to be absolutely or convectively unstable whether amplified disturbances increase in time at any fixed station and extend to the entire domain of interest or if such perturbations are transported downstream by the flow and if only the base flow remains for large time in any fixed frame). The complete phenomenon still escapes to our understanding, see Délerly [31], Sarkpaya [32], Rusak and Wang [33] for reviews. Experiments on confined vortices in tubes, e.g., Tsai and Widnall [34], confirm that vortex breakdown represents a transition from a supercritical to a subcritical flow. This transition also holds for the flow over delta wing at high angle of incidence, a popular application of vortex breakdown, see Renac and Jacquin [35]. A crude criterion for breakdown may be obtained by considering that the fastest waves travel at a speed $c \approx V_0$ (see Section 2). Criticality then leads to the following non-dimensional parameter:

$$q_c = \frac{V_0}{U_\infty + \Delta U} = \frac{q}{1.56} \frac{1}{1 + U_\infty/\Delta U} \quad (4)$$

where q is defined in (3). The flow remains supercritical (free from breakdown) if q_c is smaller than unity. Note that a supercritical vortex may remain locally stable, i.e., such that $q \geq 1.5$, thanks to the effect of the drift velocity U_∞ in (4). Note also that given Γ , breakdown condition critically depends on the core width a . This may be used to get an estimation of core width minimums. One may approximate the maximum tangential velocity by $V_0 \approx \Gamma/(2\pi a)$. In the case of trailing vortices behind wings, using an elliptic law $\Gamma = 2C_z U_0 b_0 / (\pi AR)$ for the wing loading (see any text book on aerodynamics), one obtains:

$$q_c = \frac{C_z}{AR\pi^2} \frac{b_0}{a} \frac{U_\infty}{U_\infty + \Delta U} \quad (5)$$

where C_z is the lift coefficient, AR , the wing aspect ratio, b_0 , the wing span and a , the vortex width. Typical values for a highly loaded wing are $AR = 7$, $C_z = 2$, which gives $C_z/(AR\pi^2) \approx 0.03$. With these approximations, the vortices produced by such a wing are free from breakdown ($q_c \leq 1$) whenever:

$$\frac{a}{b_0} \geq 0.03 \frac{U_\infty}{U_\infty + \Delta U} \quad (6)$$

Experiments show that trailing vortices are usually of the wake type ($\Delta U < 0$), so $a/b_0 = 3\%$ must be considered again as a minimum for a trailing wake vortex with no breakdown. This is not incompatible with known data.

The vortex breakdown phenomenon, as described above, must be distinguished from another related phenomenon called vortex bursting. Contrary to breakdown, which occurs at a definite position given a source of perturbation, burstings occur in an unpredictable way in the far-field trailing wakes, sometimes on both vortices, sometimes only on one of them. This

phenomenon is not yet completely understood. The collision of axisymmetric wavepackets has been proposed as a possible explanation by Moet et al. [36]. Other kind of catastrophic events, such as the merging between the main vortices and secondary vortex filaments, see Fig. 6(c), may also trigger it.

7. Mixing in vortices

In Section 5, we saw that a vortex with mild or large swirl number seems protected from perturbations by a stable region which develops from its periphery. In a Batchelor vortex, this ‘stabilizing buffer’ develops from $r/a \approx 2$ for $q = 0.7$ and cover the whole core when $q = 1.5$, see Fig. 9(a). This contributes to make trailing vortices particularly resistant to diffusion. This was discussed by considering a jet/vortex experiment revisited in Section 5. Another experiment which gives similar indications will be commented now. This experiment, described in [37], aimed at characterizing the mixing of jet exhausts with trailing vortices during formation of contrails behind an aircraft. It is based on the wing and the jet setup shown in Fig. 11(a). The wing span is 50 cm and the jet unit produced two small heated jets with a diameter of 1 cm. Dimensions, mean velocity and temperature are fixed to approximate similarity with typical transport aircrafts (e.g., the jets are initially 300 K above the ambience at the exit). As shown by the iso-levels of relative temperature measured by thermocouples in four sections downstream, see Figs. 11(b)–(e), the turbulent heated jets roll up around the vortex cores. They are stretched and deform by differential convection but there is no transport of temperature across the vortex periphery (in the last section temperature is sufficiently low to be considered as a passive scalar). DNS and LES simulation of this experiment or of equivalent problems have confirmed that the vortex is very resistant to mixing with the ambient flow, see Paoli and Garnier [2]. Interestingly, numerical results show that when introducing the hot jet in the vortex center, a strong confinement of the latter takes place, as in Fig. 10(b). Note that when heating the core of a vortex by this way, its intrinsic stability is reinforced by stabilizing buoyancy effects. Inversion of the temperature gradient (cold gas in the center) is destabilizing, Sipp et al. [38]. However, DNS have shown that if new instabilities develop, they quickly saturate and leave the mean vortex almost unchanged, see Coquart et al. [39]. This is another indication that vortices are very stable and resistant to diffusion.

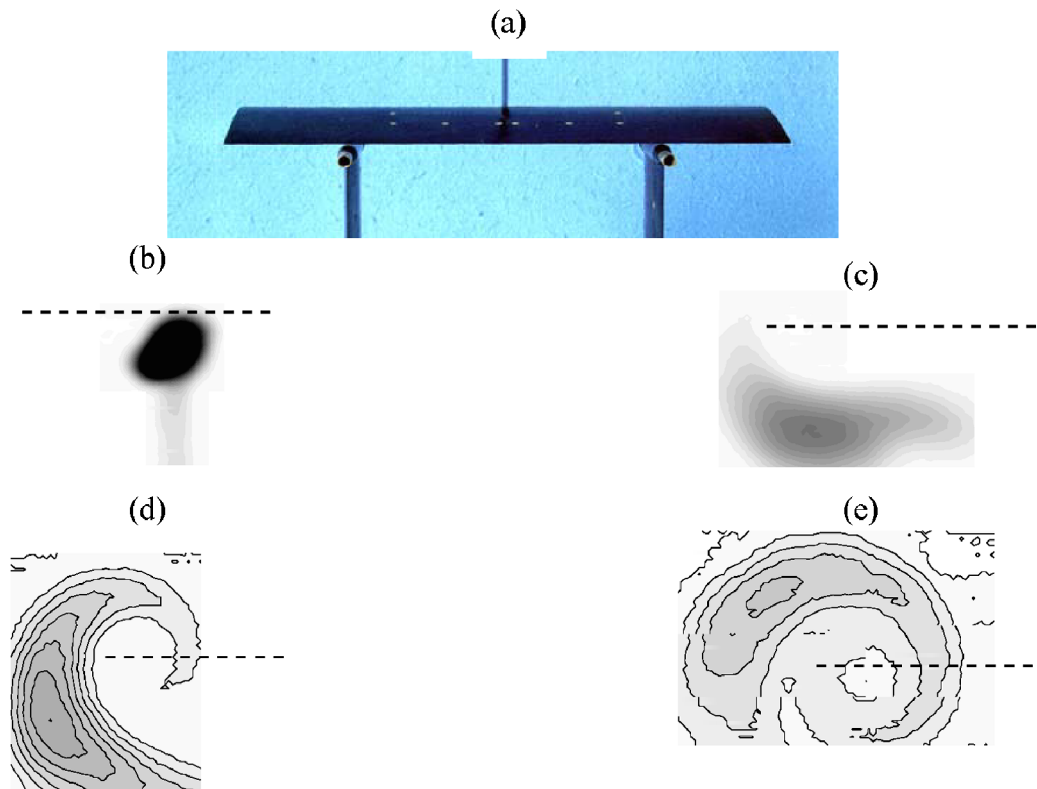


Fig. 11. Experiment on the mixing between hot jets and the trailing wake of a wing: (a) apparatus, iso-level of relative temperature at $x/b = 0.5$, (b) $x/b = 3$, (c) $x/b = 5$, (d) $x/b = 8$. The broken lines materialize the left wing tip region; the initial temperature of the jet is 600 K; from [37].

8. Vortex meandering

Vortices produced in experiments are never steady: even when separation with other vortices is sufficiently large and axial flow sufficiently weak for discarding the main instability mechanisms discussed above, one observes that vortices are always subjected to long wave and small amplitude displacements. This universal feature, called vortex meandering, still escapes our understanding. It contributes to severe measurement errors. The first comprehensive investigation of the problem has been made by Devenport et al. [40]. There are several possible causes for the phenomenon:

- (i) interference with wind tunnel unsteadiness;
- (ii) excitation of perturbations in the vortex cores by turbulence contained in the wake;
- (iii) linear co-operative instabilities;
- (iv) propagation of unsteadiness through Kelvin waves originating from the vortex generator. This list must now be updated with two other possible candidates;
- (v) viscous core instabilities;
- (vi) transient growth.

Meandering could result from a superposition of several mechanisms. Points (i) to (iv) were discussed in [41,42]. These references provide strong indications that point (i) may be discarded. Point (ii) remains open, especially if we account for point (vi) which refers to recent findings by Antkoviak and Brancher [43] on the existence of a transient growth mechanism in Lamb–Oseen vortices. Concerning point (iii), real vortices are rarely isolated and cooperative instabilities are often present (for instance, slight contributions of a cooperative instability to meandering were detected in [42]). But they do not explain meandering. Point (v) which refers to the viscous core instabilities find by Fabre and Jacquin [25], see Fig. 9(c), are more interesting because they develop for large swirl numbers, large Reynolds numbers, and they concern long wave lengths and exhibit acceptable amplification rates, see [25]. Point (iv), namely propagation of neutral Kelvin waves emanating from boundaries (aircraft), could also contribute.

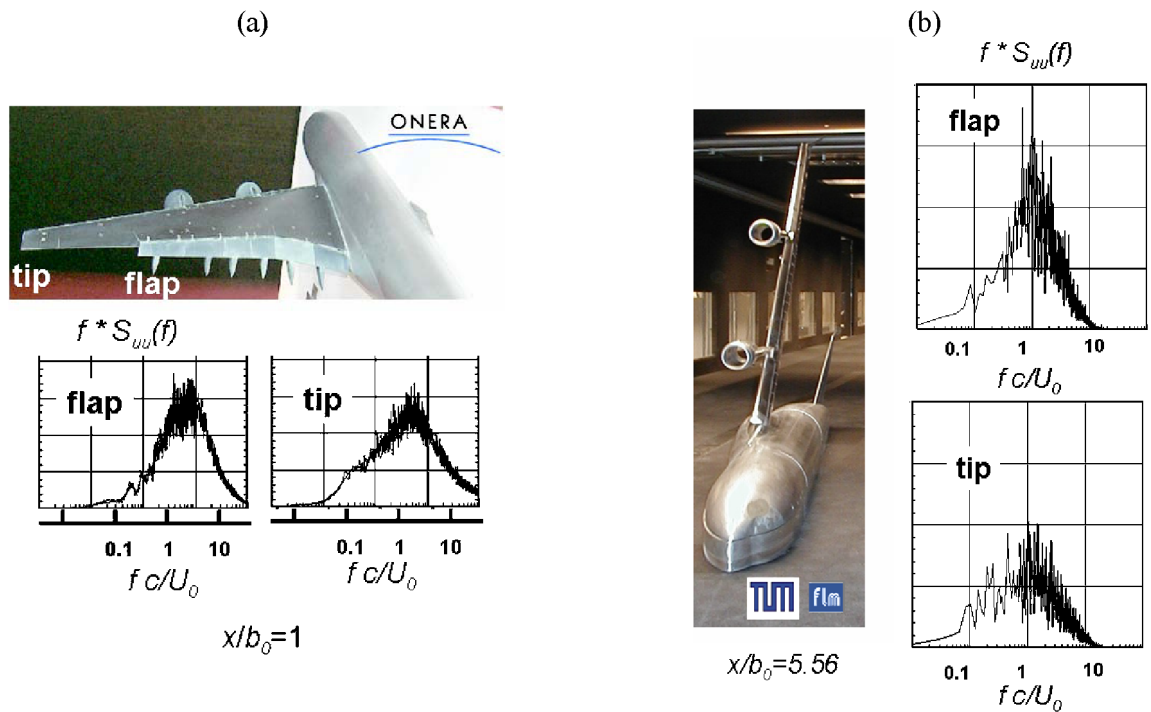


Fig. 12. Power density spectra of the axial velocity component measured with a hot wire in the centre of the wing tip and outer flap tip vortices behind two different high lifted aircraft models: (a) $x/b_0 = 1$ (experiment by ONERA), (b) $x/b = 5.56$ (experiment by the Technical University of Munchen). The spectral density $S_{uu}(f)$ is multiplied by f and it is plotted versus the frequency normalized with the wing mean chord c and the free-stream velocity. Other scales are arbitrary. See [44].

The theory of meandering remains a challenge. Fig. 12 shows an example of what must be explained. This is the typical spectral signature obtained when putting a hot wire on the axis of the vortices formed at the wing tip and at the flap tip of an aircraft model in a wind tunnel. As found in these experiments, meandering leads to broadband spectra with energy distributed around frequencies which scale on the wing chord. This result is suggesting that part of the meandering is related to the wing. Mechanisms (ii), (iv), (v) and (vi) listed above could be concerned.

9. Conclusions

As shown in this review, many results on the physics of trailing vortices are now available and are useful to appraise several important aspects of the vortex flow produced by an aircraft. Some of these results pave the way to concrete applications. This is the case of the long-wave cooperative instabilities in vortex systems which have led to propositions for the active control of aircraft wakes, see Section 3, and in the present issue, Crouch [45], Savas [14] and Winckelmanns et al. [46]. Other results, for instance those on the stability of vortices with respect to small scale perturbations, are supporting modeling strategies which are used in CFD tools, see Czech et al. [47]. They also help in understanding experimental and CFD results on the mixing between jets and vortices, as discussed in Section 7 and in the paper of Paoli and Garnier [2]. However, several problems still escape to our understanding. This is the case for meandering phenomenon, see Section 8, which received special attention due to its implications for almost all the vortex flows. Research described in this paper only provides a series of possible mechanisms which could contribute to this unsteady mechanism. Other findings described in this paper (e.g., the critical layer modes or the centre modes) are very recent and have to be explored further before concluding their possible role in the aircraft wake problem.

Acknowledgements

These research works were supported by the European Community (Brite European research programs “Eurowake” and “C-wake”), the French-Service des Programmes Aéronautiques (SPAé) and the ONERA Federated Research Project “Wake Vortex Dynamics”. These institutions are gratefully acknowledged. Part of the paper writing was funded by the EC thematic network “WakeNet2-Europe”. Jeffrey Crouch is acknowledged for reviewing the paper.

References

- [1] P. Meunier, S. Le Dizès, T. Leweke, Physics of vortex merging, *C. R. Physique* 6 (4–5) (2005), in this issue.
- [2] R. Paoli, F. Garnier, Interaction of exhaust jets and aircraft wake vortices: small-scale dynamics and potential microphysical–chemical transformations, *C. R. Physique* 6 (4–5) (2005), in this issue.
- [3] U. Schumann, Formation, properties and climatic effects of contrails, *C. R. Physique* 6 (4–5) (2005), in this issue.
- [4] P.G. Saffman, *Vortex Dynamics*, Cambridge Univ. Press, Cambridge, UK, 1992.
- [5] M. Rossi, Of vortices and vortical layers: an overview, in: A. Maurel, P. Petitjeans (Eds.), *Vortex Structures and Dynamics*, in: *Lectures in Physics*, Springer-Verlag, Berlin/New York, 2000, pp. 40–123.
- [6] D. Fabre, D. Sipp, L. Jacquin, The Kelvin waves and the singular modes of the Lamb–Oseen vortex, *J. Fluid. Mech.*, in press.
- [7] M.V. Melander, F. Hussain, Core dynamics on a vortex column, *Fluid. Dyn. Res.* 13 (1994) 1–37.
- [8] S. Arendt, D.C. Fritts, O. Andreassen, The initial value problem for Kelvin vortex waves, *J. Fluid. Mech.* 244 (1997) 181–212.
- [9] D. Fabre, *Instabilités et instationnarités dans les tourbillons—Application aux sillages d’avions*, PhD Thesis, Université de Paris 6, 2000.
- [10] S.C. Crow, Stability theory for a pair of trailing vortices, *AIAA Journal* 8 (12) (1970) 2172–2179.
- [11] J.D. Crouch, Instability and transient growth for two trailing vortex pairs, *J. Fluid Mech.* 350 (1997) 311–330.
- [12] D. Fabre, L. Jacquin, A. Loof, Optimal perturbations in a four-vortex aircraft wake in counter-rotating configuration, *J. Fluid Mech.* 451 (2002) 319–328.
- [13] J.M. Ortega, R.L. Bristol, Ö. Savas, Experimental study of the stability of unequal strength counter-rotating vortex pairs, *J. Fluid Mech.* 474 (2003) 35–84.
- [14] Ö. Savas, Experimental investigations on wake vortex and its alleviation, *C. R. Physique* 6 (4–5) (2005), in this issue.
- [15] D.W. Moore, P.G. Saffman, Motion of a vortex filament with axial flow, *Proc. R. Soc. London, Ser. A* 272 (1972) 403–429.
- [16] C. Eloy, S. Le Dizès, Stability of the Rankine vortex in a multipolar strain field, *Phys. Fluids* 13 (3) (2001) 660–676.
- [17] D. Sipp, L. Jacquin, Widnall instabilities in vortex pairs, *Phys. Fluids* 15 (7) (2003) 1861–1874.
- [18] S. Le Dizès, F. Laporte, Theoretical prediction of the elliptic instability in two vortex flow, *J. Fluid Mech.* 471 (2002) 169–201.
- [19] P. Meunier, T. Leweke, Merging and three-dimensional instability in a co-rotating vortex pair, in: A. Maurel, P. Petitjeans (Eds.), *Vortex Structure and Dynamics*, in: *Lecture Notes in Physics*, vol. 555, Springer-Verlag, Berlin/New York, 2000, pp. 241–251.
- [20] D. Sipp, Weakly non-linear saturation of short-waves instabilities in a strained Lamb–Oseen vortex, *Phys. Fluids* 12 (7) (2000) 1715–1727.
- [21] T. Leweke, H.K. Williamson, Cooperative elliptic instability of a vortex pair, *J. Fluid Mech.* 360 (1998) 85.

- [22] R.L. Ash, M.R. Khorrami, Vortex stability, in: S.I. Green (Ed.), *Fluid Vortices*, in: *Fluid Mechanics and its Applications*, vol. 30, Kluwer Academic Publishers, Dordrecht/Norwell, MA, 1995, pp. 317–372.
- [23] S. Leibovich, K. Stewartson, A sufficient condition for the instability of columnar vortices, *J. Fluid Mech.* 126 (1983) 335–356.
- [24] L. Jacquin, C. Pantano, On the persistence of trailing vortices, *J. Fluid Mech.* 471 (2002) 159–168.
- [25] D. Fabre, L. Jacquin, Viscous instabilities in trailing vortices at large swirl numbers, *J. Fluid Mech.* 500 (2004) 239–262.
- [26] W.R.C. Phillips, J.A.H. Graham, Reynolds stress measurements in a turbulent trailing vortex, *J. Fluid Mech.* 47 (1984) 353–371.
- [27] S. Ragab, M. Sreedhar, Numerical simulations of vortices with axial velocity deficit, *Phys. Fluids* 7 (1995) 549–558.
- [28] T.B. Benjamin, Theory of the vortex breakdown phenomenon, *J. Fluid Mech.* 14 (4) (1962) 593–629.
- [29] T.B. Benjamin, Some developments in the theory of vortex breakdown, *J. Fluid Mech.* 28 (1) (1967) 65–84.
- [30] F. Gallaire, J.M. Chomaz, Mode selection in swirling jet experiments: a linear stability analysis, *J. Fluid Mech.* 494 (2003) 223–253.
- [31] J. Délyery, Aspects of vortex breakdown, *Prog. Aerospace Sci.* 30 (1994) 1–59.
- [32] T. Sarkpaya, Vortex breakdown and turbulence, AIAA Paper 95-0433, in: 33rd Aerospace Sciences Meeting & Exhibit, Reno, NV, 1995.
- [33] Z. Rusak, S. Wang, Review of theoretical approaches to the vortex breakdown phenomenon, AIAA Paper 96-2126, in: 1st AIAA Theoretical Fluid Mechanics Meeting, New Orleans, LA, 1996.
- [34] C.Y. Tsai, S.E. Widnall, Examination of group-velocity criterion for breakdown of vortex flow in a divergent duct, *Phys. Fluids* 23 (5) (1980) 864–870.
- [35] F. Renac, L. Jacquin, On the linear stability properties of lifting vortices over delta wings, AIAA J., submitted for publication.
- [36] H. Moet, F. Laporte, G. Chevalier, T. Poinsot, Wave propagation in vortices and vortex bursting, *Phys. Fluids* 17 (2005), in press.
- [37] L. Jacquin, S. Brunet, P. Geffroy, Experiment on heated jets/wake vortex interaction, ONERA RT 15/2496 DAFE/Y, 1998. See also a report on this experiment in: F. Garnier, S. Brunet, L. Jacquin, Modelling exhaust plume mixing in the nearfield of an aircraft, *Annales Geophysicae*, 1997.
- [38] D. Sipp, D. Fabre, S. Michelin, L. Jacquin, Stability of a vortex with a heavy core, *J. Fluid Mech.* 526 (2005) 67–76.
- [39] L. Coquart, D. Sipp, L. Jacquin, Mixing induced by Rayleigh–Taylor instability in a vortex, *Phys. Fluids*, in press.
- [40] W.J. Devenport, M.C. Rife, S.I. Liaps, G.J. Follin, The structure and development of a wing tip vortex, *J. Fluid Mech.* 312 (1996) 67–106.
- [41] L. Jacquin, D. Fabre, D. Sipp, H. Vollmers, V. Theofilis, Instability and unsteadiness of aircraft vortex wakes, *Aerospace Sci. Technol.* 7 (8) (2003) 577–593.
- [42] L. Jacquin, D. Fabre, P. Geffroy, E. Coustols, The properties of a transport aircraft wake in the extended near-field, AIAA paper No 2001-1038, 2001.
- [43] A. Antkowiak, P. Brancher, Transient energy growth for the Lamb–Oseen vortex, *Phys. Fluids* 16 (2004) 1–4.
- [44] K. Hünecke, C-wake, wake vortex characterisation and control, Final report, 2003.
- [45] J. Crouch, Airplane trailing vortices and their control, *C. R. Physique* 6 (4–5) (2005), in this issue.
- [46] G. Winckelmans, R. Cocle, L. Dufresne, R. Capart, Vortex methods and their application to trailing wake vortex simulations, *C. R. Physique* 6 (4–5) (2005), in this issue.
- [47] M. Czech, G. Miller, J. Crouch, M. Strelets, Predicting the near-field evolution of airplane trailing vortices, *C. R. Physique* 6 (4–5) (2005), in this issue.